Ultrafast magnetization dynamics in magnetic tunneling junctions

Xiaojing Zou and Gang Xiao

Ultrafast magnetization dynamics in magnetic tunneling junctions

Xiaojing Zou[1,a)] and Gang Xiao[2,b)]
[1]*Micro Magnetics, Inc., 617 Airport Road, Fall River, Massachusetts 02720, USA*
[2]*Department of Physics, Brown University, Providence, Rhode Island 02912, USA*

To understand the dynamic magnetic properties and its relationship to ultrafast field sensing, we performed micromagnetic simulations on actual MgO-based magnetic tunneling junction (MTJ) structures. The results indicate that an MTJ with a larger aspect ratio yields a smaller response time under a sudden change of an external magnetic field. Such an effect is mainly due to the coherent rotation from the central cores inside the junction element. Damping coefficient is shown to play an important role in ultrafast sensing and the optimal value need to be a few times larger than typical values found in common ferromagnetically soft materials. Our calculations further show that the response time can be reduced by increasing the free layer thickness and/or its saturation magnetization. Finally, we have obtained the dependence of intrinsic resonance frequency on the sensor size while keeping the same aspect ratio. © *2011 American Institute of Physics*. [doi:10.1063/1.3605557]

Ultrafast magnetization dynamics in magnetic tunneling junctions (MTJs)[1–3] is an important topic in the field of spintronics, as MTJs have been used both in speedy non-volatile magnetic random access memories (MRAMs)[4] and in high frequency magnetic sensors.[5–7] In MRAMs, the dynamics pertains to large angle magnetization rotations.[8] In sensing applications, however, the magnetization vector undergoes very small angular responses to the weak external field. The potential for ultrafast speed is a significant advantage of MTJs in comparison with other magnetic devices, such as fluxgates or SQUIDs (superconducting quantum interference devices). Till now much of the research on the dynamic properties of MTJs is related to magnetization reversal, studies focusing on the ultrafast sensing are rare. Hence, in this Letter, we will investigate the ultrafast dynamic response of MTJs in various geometrical dimensions (aspect ratio, size, and free-layer thickness) and intrinsic physical parameters (damping coefficient and saturation magnetization).

The basic MTJ structure used in our simulation is a typical magnetic sensor layer structure: CoFe(20)/Ru(8)/CoFeB(30)/MgO(20.5)/CoFeB(t_{free}) (thickness unit in Å).[9,10] The bottom ferromagnetic(FM) film CoFeB(30) is exchange coupled to the CoFe(20) layer, which is made into a pinned layer with magnetization along the Y-axis. MgO(20.5) serves as the tunneling barrier and the top FM film CoFeB(t_{free}) is the free-layer whose dynamical properties are the focus of this study.

The dynamic micromagnetic model we developed is based on the Landau-Lifshitz-Gilbert (LLG) equation

$$\frac{\partial M}{\partial t} = -\gamma M \times \mathbf{H}_{\text{eff}} + \frac{\alpha}{M_s} M \times \frac{\partial M}{\partial t}, \qquad (1)$$

where γ is the gyromagnetic factor and α is the Gilbert damping coefficient. The effective magnetic field $\mathbf{H}_{\text{eff}}$ is determined by the energy variational with magnetization $\mathbf{H}_{\text{eff}} = -\partial E/\partial \mathbf{M}$, where E is the total energy of the system. Our

micromagnetic simulation modeled the above MTJ structure as three FM layers that each was composed of numerous square cells with identical size ranging from 5 nm to 50 nm. The total energy E is calculated as the summation of the magnetostatic, anisotropy, interlayer exchange coupling, and Zeeman energy terms from the three FM layers as a whole. The typical material parameters are[11–14]: exchange stiffness constant $A_{CoFeB} = 2.5 \times 10^{-6}$ erg/cm and $A_{CoFe} = 3.0 \times 10^{-6}$ erg/cm, saturation magnetization $M_{s(CoFeB)} = 1200$ emu/cm^3 and $M_{s(CoFe)} = 1900$ emu/cm^3, and uniaxial anisotropy constant $K_{1(CoFeB)} = 1.4 \times 10^4$ erg/cm^3 with anisotropy directions randomly distributed among the small square cells.

In the simulations, a large external field is first applied along the Y-axis direction to saturate the sample, then this magnetic field is gradually decreased to zero and the current magnetization configuration is in the remanent state. Finally, a small step function magnetic field is applied along the sensing direction (Y-axis in our case) and the evolution of magnetization is determined by numerically solving the LLG equation.

Figs. 1(a)–1(c) show the simulated time dependence of the magnetization in Y direction (m_y) for sensors with different junction heights after applying an external field along Y axis ($H_y = 1$ Oe). The width of the junctions is all fixed at 6.0 μm, and the damping constant α is assumed to be 0.02. As can be seen in Fig. 1(a), for sensor with a height of 0.75 μm, m_y oscillates in time with a decaying amplitude and reaches a final stable state after certain amount of time. As the junction height increases, the oscillating feature weakens significantly at 3.0 μm and eventually disappears at a height of 6.0 μm in Fig. 1(c), where the magnetization approaches the final stable value asymptotically.

Based on Figs. 1(a)–1(c), we can define a response time τ for each case, which reflects the time required to reach the final stable state. τ is determined by reversely identifying the first data point that yield a deviation from the final state larger than one percent of the total change in m_y, i.e., $\Delta m_y > 1\% \cdot |m_{y(\text{final})} - m_{y(t=0)}|$. We plotted in Fig. 1(d) the response time as a function of the aspect ratio of the MTJ sensor with

a)Electronic mail: Zou@micromagnetics.com.
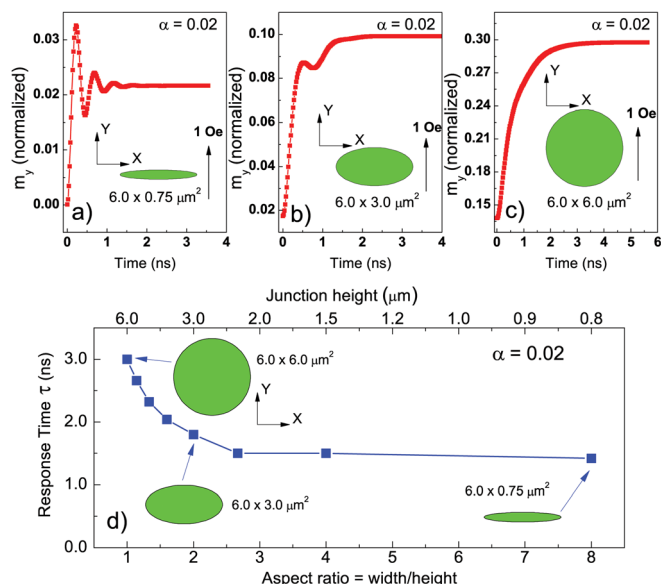b)Electronic mail: Gang_Xiao@brown.edu.

FIG. 1. (Color online) Simulated magnetic moment (m_y, normalized) versus the elapsed time (in nanosecond), after applying $H_y = 1$ Oe (step) to MTJ sensors with different heights: (a) 0.75 μm, (b) 3.0 μm, and (c) 6.0 μm, but a fixed width of 6.0 μm. (d) Response time τ as a function of the MTJ aspect ratio. In all simulations, the damping coefficient α is held at 0.02.

a constant width of 6.0 microns. The response time can be reduced by a factor of 2 as the shape is changed from a circle with high symmetry to an elongated ellipse.

To better understand the physical mechanism leading to the shape dependence shown above, we display in Fig. 2 the simulated images of magnetization pattern before and after turning on the external field ($H_y = 1$ Oe). In the case of a large aspect ratio, e.g., for the 6.0×0.75 μm^2 MTJ shown in Fig. 2(a), the magnetization vector is uniform and aligned mainly along the x-axis, without any existence of a domain

wall. Upon applying an external field of 1 Oe, the magnetic moments rotate only minutely, implying the existence of a large internal field $\mathbf{M}_{\mathrm{eff}}$, which prevents the magnetic moments from moving toward the external field direction.

As the aspect ratio is reduced, as in Fig. 2(b), there appear some small edge domains that do not respond to the external field easily (see m_x maps). Rather, the response to external field is primarily from the visible expansion and coherent rotation of two cores near the central region of the MTJ as seen in the m_y maps. This indicates that the effective internal field has been weakened from the case with a large aspect ratio as shown in Fig. 2(a). Finally, in the most symmetrical circular MTJ shown in Fig. 2(c), the central core expands and rotates easily in response to an external field, particularly visible in the m_y maps, implying that the effective internal field has been minimized among three shapes in Fig. 2.

The results shown in Figs. 1 and 2 are consistent with the general relation between the response time τ and the effective internal field: $\tau \propto 1/\mathbf{M}_{\mathrm{eff}}$, where α is the damping coefficient.[15] Hence, a stronger effective internal field is beneficial to ultrafast magnetic sensing.

Next, we study the dependence of response time τ on free-layer thickness t_{free}, saturation magnetization M_s, and damping coefficient α. We have selected one particular shape (6.0×0.75 μm^2), which yields the smallest response time because of its large aspect ratio. The two-dimensional response time map is shown in Fig. 3(a) as a function of t_{free} and α, and in Fig. 3(b) of M_s and α. For ultrafast sensing, the material parameters (t_{free}, M_s, and α) should be chosen within the shaded deep blue area, which corresponds to the smallest response time section ($\tau < 0.4$ ns). It is clear that once the damping factor α is fixed, thicker free-layers and/or larger M_s are beneficial to fast response. Generally speaking, the damping coefficient plays an important role in the response
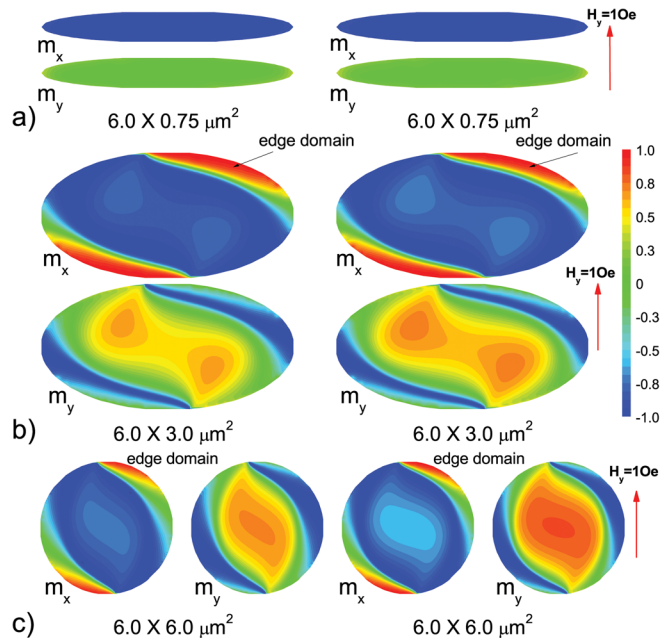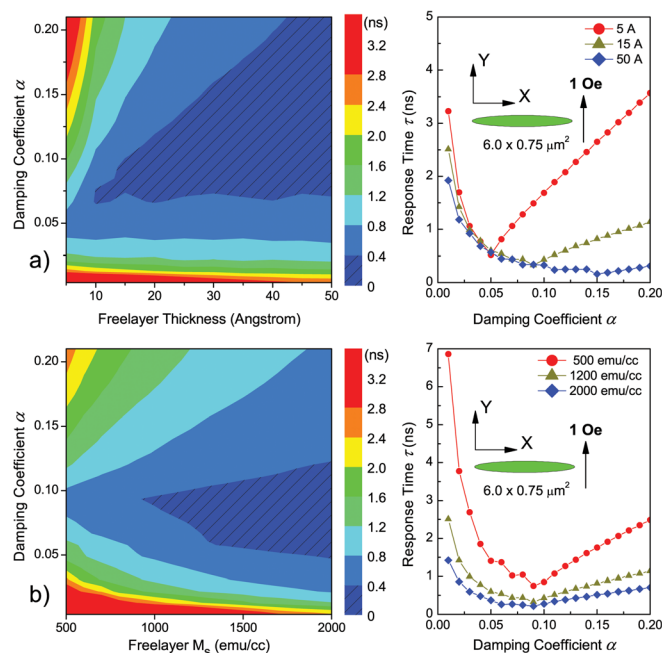

FIG. 2. (Color online) Simulated magnetization (m_x and m_y) distribution, before and after the application of $H_y = 1$ Oe (step), for three types of MTJ sensors with different heights: (a) 0.75 μm, (b) 3.0 μm, and (c) 6.0 μm, but a fixed width of 6.0 μm. The color bar indicates the magnitude of m_x and m_y. The damping coefficient α is held at 0.02 in all simulations.

FIG. 3. (Color online) (a) Response time τ in a color-coded map as a function of both free-layer thickness t_{free} and damping coefficient α. (b) Response time τ as a function of both free-layer saturation magnetization M_s and damping factor α.
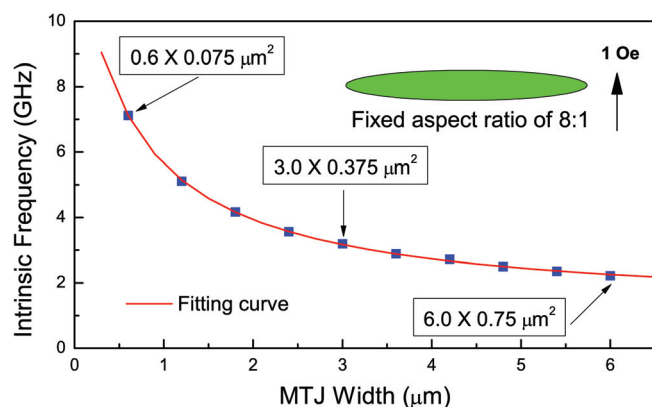
FIG. 4. (Color online) MTJ size dependence of the intrinsic ferromagnetic resonance frequency f_0. These junctions have the same aspect ratio of 8:1 but different width ranging from 0.6 μm to 6.0 μm. Both the free-layer thickness t_{free} and damping coefficient α are held constantly at 15 Å and 0.02 in the micromagnetic simulations.

time. As evidenced in the right panel of Fig. 3, for a given thickness or M_s, there always exists an optimal α_0 for the shortest response time, and this α_0 is typically in the range from 0.05 to 0.09. The magnetization motion is under-damped when $\alpha < \alpha_0$ and overdamped when $\alpha > \alpha_0$, resulting in an abrupt slope change around the optimal damping value.

Finally, we studied the effect of MTJ's geometrical size on the magnetic dynamics. For high frequency magnetic sensing, the maximum frequency limit is the intrinsic ferro-magnetic resonance frequency f_0 of the MTJ. Fig. 4 plots the f_0 as a function of the junction size with a constant aspect ratio of 8:1. The free-layer thickness and damping coefficient is held at 15 Å and 0.02. As the size is reduced, f_0 increases from 2.2 to 7 GHz for the smallest MTJ (0.6×0.075 μm^2). The best fitting curve using reciprocal function yields a $f_0 \rightarrow 1.2$ GHz for very large sensor, which is quite consistent with the experimental observations on thin CoFeB films.[16,17] Fig. 4 shows that for ultrafast sensing MTJ sensors should be fabricated in the sub-micron scale, which yields a high f_0.

In summary, micromagnetic simulations on practical MTJ sensor structures have shown the existence of an opti-mal damping coefficient α for a minimum response time. The value is a few times larger than the typical values of

commonly used soft ferromagnetic thin films. Furthermore, given α, an MTJ with a sub-micron dimension and a larger aspect ratio is better suitable for ultrafast magnetic sensing. We have also found that thicker free-layer and larger mag-netization will reduce magnetic response time.

[1]S. Parkin, C. Kaiser, A. Panchula, P. Rice, B. Hughes, M. Samant, and S. Yang, Nature Mater. **3**, 862 (2004).

[2]S. Yuasa, T. Nagahama, A. Fukushima, Y. Suzuki, and K. Ando, Nature Mater. **3**, 868 (2004).

[3]J. S. Moodera, J. Nassar, and G. Mathon, Annu. Rev. Mater. Sci. **29**, 381 (1999).

[4]S. Ikeda, J. Hayakawa, Y. M. Lee, F. Matsukura, Y. Ohno, T. Hanyu, and H. Ohno, IEEE Trans. Electron Devices **54**, 991 (2007).

[5]K. Tsunekawa, D. D. Djayaprawira, M. Nagai, H. Maehara, S. Yamagata, N. Watanabe, S. Yuasa, Y. Suzuki, and K. Ando, Appl. Phys. Lett. **87**, 072503 (2005).

[6]P. P. Freitas, R. Ferreira, S. Cardoso, and F. Cardoso, J. Phys.: Condens. Matter **19**, 165221 (2007).

[7]S. Ingvarsson, M. Arikan, M. Carter, W. F. Shen, and Gang Xiao, Appl. Phys. Lett. **96**, 232506 (2010).

[8]R. H. Koch, J. G. Deak, D. W. Abraham, P. L. Trouilloud, R. A. Altman, Y. Lu, W. J. Gallagher, R. E. Scheuerlein, K. P. Roche, and S. S. P. Parkin, Phys. Rev. Lett. **81**, 4512 (1998).

[9]W. F. Shen, D. Mazumdar, X. J. Zou, X. Y. Liu, B. D. Schrag, and Gang Xiao, Appl. Phys. Lett. **88**, 182508 (2006).

[10]W. F. Shen, B. D. Schrag, A. Girdhar, M. J. Carter, H. Sang, and Gang Xiao, Phys. Rev. B **79**, 014418 (2009).

[11]A. Ney, C. Pampuch, R. Koch, and K. H. Ploog, Nature **425**, 485 (2003).

[12]A. Lyle, X. F. Yao, F. Ebrahimi, J. Harms, and J. P. Wang, IEEE Trans. Magn. **46**, 2216 (2010).

[13]S. B. Choe, Y. Acremann, A. Scholl, A. Bauer, A. Doran, J. Stohr, and H. A. Padmore, Science **304**, 420 (2004).

[14]B. D. Cullity and C. D. Graham, Introduction to Magnetic Materials, 2nd ed. (Wiley, New York, 2008).

[15]C. Kittel, Introduction to Solid State Physics, 8th ed. (Wiley, New York, 2004).

[16]G. D. Fuchs, J. C. Sankey, V. S. Pribiag, L. Qian, P. M. Braganca, A. G. G. Garcia, E. M. Ryan, Z.-P. Li, O. Ozatay, D. C. Ralph, and R. A. Buhr-man, Appl. Phys. Lett. **91**, 062507 (2007).

[17]C. Bilzer, T. Devolder, Joo-Voo Kim, G. Couinl, C. Chappert, S. Cardoso, and P. P. Freitas, J. Appl. Phys. **100**, 053903 (2006).